

An Anderson Impurity Model for Efficient Sampling of Adiabatic Potential Energy Surfaces of Transition Metal Complexes

M.X. LaBute^{1,3}, R.G. Endres^{2,3}, and D.L. Cox³

Theoretical Division, Los Alamos National Laboratory, Los Alamos, NM 87545, USA¹

Center for Computational Sciences & Computer Science and Mathematics Division,

Oak Ridge National Laboratory, Oak Ridge TN 37831-6164, USA²

Department of Physics, University of California, Davis, CA 95616, USA³

(Dated: August 28, 2018)

We present a model intended for rapid sampling of ground and excited state potential energy surfaces for first-row transition metal active sites. The method is computationally inexpensive and is suited for dynamics simulations where (1) adiabatic states are required "on-the-fly" and (2) the primary source of the electronic coupling between the diabatic states is the perturbative spin-orbit interaction among the $3d$ electrons. The model Hamiltonian we develop is a variant of the Anderson impurity model and achieves efficiency through a physically motivated basis set reduction based on the large value of the d - d Coulomb interaction U_d and a Lánczos matrix diagonalization routine to solve for eigenvalues. The model parameters are constrained by fits to the partial density of states (PDOS) obtained from *ab initio* density functional theory calculations. For a particular application of our model we focus on electron-transfer occurring between cobalt ions solvated by ammonium, incorporating configuration interaction between multiplet states for both metal ions. We demonstrate the capability of the method to efficiently calculate adiabatic potential energy surfaces and the electronic coupling factor we have calculated compares well to previous calculations and experiment.

I. INTRODUCTION

First-row transition metals (TM) complexed with organic ligands play key roles in biology and aqueous chemistry. Ligand exchange and electron transfer are potentially rate-limiting processes that must be considered in industrial or bio-remedial chemistry [1]. Ligand binding at the iron porphyrin active sites of heme proteins are fundamental for oxygen transport and aerobic metabolism [2]. Many of these reactions involve non-radiative transitions between different spin states and require spin-orbit coupling. This interaction occurs primarily on the TM atom due to the localized nature of the $3d$ valence electrons and most quantum chemistry codes do not incorporate the small (~ 0.05 - 0.1 eV) energy-scale coupling.

In general, treatment of open-shell TM atoms is difficult and many of the standard density-functional theory (DFT) model chemistries such as the local density or gradient-corrected approximations (LDA and GGA, respectively) are known to give erroneous qualitative results in some cases [3]. The primary source of these problems are *non-dynamical correlations* associated with the near-degeneracy of configurations with the Hartree-Fock single-Slater determinant groundstate [4]. In fact, it is clear that in the vicinity of the transition state of a charge transfer complex such *non-dynamical correlations* may be very important, much as they are in chemical bond breaking. One may incorporate these effects by higher-order corrections such as Moller-Plesset perturbation theory (MP2,MP4) or configuration interaction (CI) methods such as complete active space self-consistent field (CASSCF), or, especially for non-dynamical correlations, multireference configuration interaction approaches[5],

but these methods are computationally prohibitive for TM molecules containing ~ 50 atoms. In many cases the CI must be limited to single excitations, which may be insufficient[6].

While the addition of some amount of non-local exchange used in the hybrid Hartree-Fock/DFT methods such as B3LYP seems to capture some of the multi-determinantal character of TM systems [7, 8, 9], the minimal local Gaussian basis sets required for quantitative accuracy are very large and the sampling required for dynamics and the calculation of excited states is not yet affordable for most processors.

In this paper we introduce an effective semi-empirical model Hamiltonian that is well-suited for (~ 50 - 100 atoms) TM molecules. The problematic aspect of strongly correlated TM systems, the (d - d Coulomb interaction), leads to a physically-motivated reduction of the many-body basis set required by limiting the number of d^n configurations that must be considered. We develop a variant of the Anderson Impurity Model (AIM), which has had some success in describing spectra and energetics of TM solid-state systems [10]. We then describe our method of solving for the groundstate of this model using the variational *ansatz* for the groundstate wavefunction of Gunnarsson and Schönhammer [11] and Varma and Yafet [12]. The AIM reduces the multiple-degrees of freedom of this problem to a small number of one-electron and Coulomb input parameters. We show how these parameters can be constrained and, in some cases, directly extracted from *ab initio* DFT calculations. We have done this using the SIESTA [13] code. The tensor product basis formed from the TM $3d$ and ligand orbitals results in a very large eigenvalue problem. We solve for ground and excited states with an efficient Lánczos diag-

onalization routine. This model, which is similar to the angular-overlap model of Gerloch and co-workers [14], differs in both the physically-motivated truncation of the basis set and also in the method of parameterization. We seek here to identify the *microscopic* origin of model parameters that describe the electronic structure, such as the d - d Coulomb repulsion and the ligand-field splitting, rather than focusing on structural sensitivities [15]

We now develop the model in detail and apply it to the electron transfer reaction between $Co(NH_3)_{6(aq)}^{2+}$ [Co(II)] and $Co(NH_3)_{6(aq)}^{3+}$ [Co(III)] molecules in solution, which has been extensively investigated by *ab initio* electronic structure methods [16, 17, 18].

II. THE MODEL

The TM molecules we wish to investigate are typically composed of a single $3d$ TM atom bound to one or more ligands. We express the model Hamiltonian in 2nd-quantized notation using the $3d$ atomic orbitals of the TM atom and the molecular orbital eigenstates of the ligands. We have recently applied a similar model to the study of the electronic structure of cobalt valence tautomers [19].

The electron correlation effects that we wish to incorporate into our model result from the localized character of the atomic $3d$ -orbitals on the TM atom. The ligand molecular orbitals will tend to be more delocalized over several atomic sites. A set of localized atomic levels hybridized to a reservoir of more extended electronic states is well-described by an Anderson Impurity Model. We may write down a variant of this model, specific for TM molecules:

$$\begin{aligned}
 H = & \epsilon_L \sum_{j\sigma} c_{j\sigma}^\dagger c_{j\sigma} + \sum_{\gamma\sigma} [\epsilon_{d\gamma\sigma} - g_\gamma x] d_{\gamma\sigma}^\dagger d_{\gamma\sigma} \quad (1) \\
 & + \sum_{\substack{\gamma, i \\ \sigma^i}} V_{\gamma i} (c_{i\sigma}^\dagger d_{\gamma\sigma} + h.c.) + U_d \sum_{\gamma\sigma > \gamma'\sigma'} n_{\gamma\sigma} n_{\gamma'\sigma'} \\
 & + J_d \sum_{\gamma\sigma > \gamma'\sigma'} \vec{s}_{\gamma\sigma} \cdot \vec{s}_{\gamma'\sigma'} + \sum_{i=1}^{N_d} \xi(\vec{r}) \vec{l}_i \cdot \vec{s}_i \\
 & + \frac{1}{2} \sum_{\substack{i \neq j \\ \sigma}} V_{ij} (c_{i\sigma}^\dagger c_{j\sigma} + h.c.) + \frac{1}{2} K x^2
 \end{aligned}$$

where ϵ_{Li} are the on-site energies for the redox-active ligand molecular orbitals and $c_{j\sigma}^\dagger$ are the corresponding fermion creation operators for the ligand molecular orbitals. The operator $d_{\gamma\sigma}^\dagger$ creates an electron in the TM $3d$ -orbital with O_h symmetry label $\gamma = xy, yz, xz, 3z^2 - r^2, x^2 - y^2$ and σ spin. $V_{\gamma i}$ are the hopping matrix element between the Co $3d$ -orbitals and the ligand states. We also include the $3d$ spin-orbit (s.o.) in its first-order

perturbative form. The inclusion of the TM s.o. is significant for processes that involve changes in the total spin of the electrons in the $3d$ shell.

Given the large changes in reorganization energy that can accompany these processes, we need to couple our model, which deals only with the valence electronic sector, to a relevant reaction coordinate, such as bond length change. This is especially vital for biomolecules where function is modulated by structural changes [20]. The simplest way to couple the TM molecule to the environment is via the terms in Eqn.(4): The term $g_\gamma x d_{\gamma\sigma}^\dagger d_{\gamma\sigma}$ provides a (Holstein) linear coupling of the d -level charge occupancy of the TM atom and the reaction coordinate, the change in metal-ligand bond distance, x . At lowest order, the potential energy surfaces are harmonic and so we can add an energy term that is parabolic in x : $(1/2)Kx^2$. The linear coupling and the parabolic energy term can both be obtained from a gradient expansion of the hybridization about the M-L bond length minimum [21]:

$$\begin{aligned}
 V(x) = & V(x)|_{x=x_0} + \frac{\partial V}{\partial x} \Big|_{x=x_0} (x - x_0) + \quad (2) \\
 & \frac{1}{2!} \frac{\partial^2 V}{\partial x^2} \Big|_{x=x_0} (x - x_0)^2 + \dots
 \end{aligned}$$

where $V(x)|_{x=x_0} = V_{\gamma\sigma}$, the linear coupling $\frac{\partial V}{\partial x} \Big|_{x=x_0}$ we estimate by taking the first derivative of the appropriate Slater-Koster integral [22], using a distance-parameterized expression [23],

$$-g := \frac{\partial V}{\partial x} \Big|_{x=x_0} \simeq \frac{\partial V_{pd\sigma}}{\partial x} \Big|_{x=x_0} = \eta_{pd\sigma} \frac{-7 \hbar^2 r_d^{3/2}}{2 m x^{9/2}} \Big|_{x=x_0} \quad (3)$$

where x_0 is the equilibrium bond length. This expression should be valid for small displacements away from x_0 and weak coupling between the TM d -electrons and changes in M-L bond length. From a simple harmonic oscillator model K is related to the single-active metal-ligand stretching mode ω by $\omega = \sqrt{K/M}$ where M is the reduced mass which may be approximated by the total mass of all six NH_3 ligands. To obtain K we refer to experimental metal-ligand vibrational data [24].

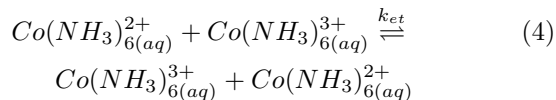
We now show how we apply this model to a particular system, the self-exchange electron-transfer in the cobalt hexaammines, $Co(NH_3)_{6(aq)}^{2+/3+}$.

III. ELECTRON-TRANSFER IN $Co(NH_3)_{6(aq)}^{2+/3+}$

A. Experimental and Theoretical Review

We would like to examine how effects arising from strong correlations manifest in the general problem of electron transfer between solvated 1st-row transition metal ions that are mediated by a ligand bridge. In particular, we focus on the electron self-exchange rate in

the cobalt hexaammine system $Co(NH_3)_6^{2+/3+}$, which is given by the following reaction:



and the reasons why k_{et} is two orders of magnitude larger than predicted. Experimental measurements of the rate ($k_{et} \sim 10^{-6}$ - 10^{-5} $M^{-1}s^{-1}$) [25] deem the reaction adiabatic, i.e. where the electron transmission coefficient $\kappa \approx 1$, while previous theoretical efforts ($k_{et} \sim 10^{-8}$ $M^{-1}s^{-1}$) yield $\kappa_{el} \ll 1$ [26]. Electronic structure effects can be important for ET between small TM complexes in solution (which we define to be the metal ion and the six coordinating ligands of the first solvation shell) that are in contact with each other. In the case of the hexaamines, the salient feature appears to be a "spin barrier", (first pointed out by Orgel [27]). During the course of the transfer process, each cobalt ion must change its spin by $\Delta S = 3/2$. Strictly speaking, k_{et} should be zero, but various schemes have been proposed to show why the rate is, in fact, almost adiabatic.

The model for the electron-transfer process is usually treated as two cobalt ions (one Co(II) valence, the other Co(III)) that are each surrounded by their primary solvation shells which consist of six octahedrally-coordinated NH_3 groups. The ET between the $Co(NH_3)_6^{2+/3+}$ complexes is generally believed to be an outer-sphere process, so the ligands act as a bridge that the tunnelling electron delocalizes over during the reaction. The redox-active orbitals of the ammine ligands are the highest occupied molecular orbitals (HOMOs) of the amines which have σ symmetry and hybridize strongly with the cobalt e_g orbitals [28]. The strong σ -donating ability of the ammine ligand has been confirmed by NMR studies which observe the kinetic stability of this complex through the rate of water exchange of $Co(NH_3)_6^{2+/3+}$. This rate for $Co(NH_3)_6^{2+/3+}$ is a factor of $\sim 10^6$ slower than for $Co(H_2O)_6^{2+/3+}$ [1].

The ET reaction can be reduced to a unimolecular process by consideration of the encounter complex, which is formed by the van der Waals contact of the two primary coordination shells of the metal ions. This can be done in a variety of orientations [29]. The two most commonly considered are the (1) apex-to-apex, which involves contact along the C_4 axis, and is the most optimal bridge since the $1s$ orbitals of the hydrogen atoms of the two amines in close-contact show large mixing, and (2) face-to-face, which has two faces perpendicular to the C_3 body-diagonal. The ammine contact is probably not as good here but there are 6 amines in contact instead of 2. For calculation of k_{et} and H_{DA} , some averaging over different orientations should be done to give a more realistic estimates of these quantities. We do not do that here, only focusing on the most optimal geometry, apex-to-apex. Given this fixed geometry, we investigate electronic structure effects.

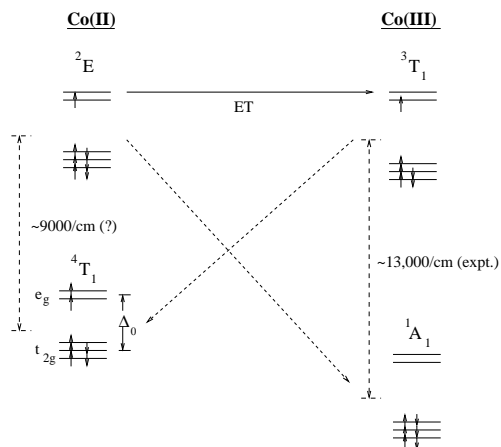


FIG. 1: Lowest energy configurations and excited states for Co^{2+} and Co^{3+} valences. These are the relevant electronic states for the self-exchange electron transfer reaction between cobalt atoms in $Co(NH_3)_6^{2+/3+}$. The question mark in the Co^{2+} excited state refers to an estimate by Buhks, *et al.* at the equilibrium configuration.

Buhks *et al.* [26] first noted that the groundstate-to-groundstate electron-transfer between the low-spin $Co(III)$ ion ($3d^6$)($1A_1$) and the high-spin $Co(II)$ ion ($3d^7$)($4T_1$) is spin-forbidden and the reaction must proceed through the $S = 1/2$ $2E$ excited state for $Co(II)$ or the $S = 1$ $3T_1$ and $3T_2$ of $Co(III)$. They also showed that there is a non-zero s.o. coupling matrix element between these ground and excited states, so the groundstates are not single-determinant but show small admixture to these excited states. Thermal population of these excited configurations is an open issue [16, 17, 18]. The vertical energy separation between $1A_1$ and $3T_1$ for $Co(III)$ is very large ($\sim 14,000$ cm^{-1}) and well-established by experiment. On the other hand, the separation between $4T_1$ and $2E$ for $Co(II)$ has been estimated from semi-empirical INDO/CI calculations to be 3000 - 9000 cm^{-1} [16]. While the existence of low-spin $Co(III)$ has been experimentally verified, no such confirmation exists for high-spin $Co(II)$. Thus, appreciable population of the $2E$ may yet be a viable possibility. Also, it should be noted that these values have been estimated for the equilibrium configuration. The relevant values for the energy separation should be made at the transition state, where they will be significantly reduced. This discussion is summarized in Fig.(1).

Other theoretical work, most notably by Newton [28] and Sutin [30], who used *ab initio* self-consistent field, spin-restricted Hartree-Fock to calculate the electronic coupling matrix element H_{DA} , assumed $2E$ as the $Co(II)$ groundstate. Newton obtained a value of 940 cm^{-1} for the spin-allowed electron transfer. He then used a reduction factor of 2×10^{-2} to account for the 2^{nd} -order spin-orbit coupling, obtaining a value of 20 cm^{-1} for the $4T_1$ to $1A_1$ process which corresponds to a $\kappa \simeq 4.0 \times 10^{-3}$.

Furthermore, Newton considered different orientations for the encounter complex, such as apex-to-apex, edge-to-edge, and face-to-face, which will alter hybridization-matrix elements and differ in the number of bridging ligands (2, 4, 6, respectively).

Newton, in a more recent paper [18], calculated the relative energies of 4T_1 and 2E electronic configurations of Co(II) and the 1A_1 , 3T_1 of Co(III) using unrestricted Hartree-Fock (UHF) and second-order Møller-Plesset (UMP2). He recalculated H_{DA} and κ for the apex-to-apex geometry using these semi-empirical CI methods that take into account electron correlations at the level of 2nd-order Brillouin-Wigner perturbation theory. For the groundstate pathway, ${}^4T_1/{}^1A_1 \rightarrow {}^1A_1/{}^4T_1$ he obtains a values ($H_{DA} = 9.5 \text{ cm}^{-1}$, $\kappa = 1.2 \times 10^{-3}$) which are optimal in the sense that the $3z^2 - r^2 - \text{NH}_3$ σ -HOMO hybridization can only decrease in other geometries. He estimates the effect of orientational averaging by taking into account a multiplicative factor 0.1; $\bar{\kappa}_{el} \sim 0.1(\kappa_{el})_{\text{apex-to-apex}}$ so $\bar{\kappa}_{el} \sim 10^{-4}$, still falling 2 orders of magnitude short of explaining the observed results.

B. Many-Electron Basis Set

We use the model Hamiltonian of Eqn.(1), which involves use of an *ansatz* for the groundstate wavefunction with the coefficients to be determined variationally. The wavefunction is composed of the lowest-lying single-determinants in the many-electron Hilbert space, where the truncation of the space is dictated by energetics. Our problem therefore reduces to diagonalizing the model Hamiltonian in a restricted Hilbert space. We first considered the two nominal valences for each cobalt hexammine reactant. In each case the most significant states are the high-spin and low-spin state, the spin-orbit excited states, and states that couple by hole transport to the bridging NH_3 HOMO. For $\text{Co}(\text{NH}_3)_6^{2+}$ we use the groundstate 4T_1 , which is the three-fold degenerate $hs-3d^7$. The spin-orbit state is, as stated above, $ls-3d^7$. Each of the manifolds couples to respective hole-transfer states which are labeled by O_h irreps of the $3d$ electron sector 3A_2 , 1A_1 , 1E , 3T_1 , and 3T_2 of the $3d^8$ configuration on the cobalt atom. Due to suppression of d^9 occupancy by U_d , we restrict the Hilbert space to the one-hole sector on the ligands. The states we retain as our basis gives a total of 65 states.

For $\text{Co}(\text{NH}_3)_6^{3+}$, we consider the following $3d^6$ states: The experimentally observed groundstate configuration 1A_1 , and the states that couples via spin-orbit coupling 3T_1 , 3T_2 . We would like to observe the suppression of the d^8 configuration, so we include many more hole-transfer states for this calculation. For the $3d^7 \underline{L}$ states we have 2E and 4T_1 . We also include the two-hole states ($3d^8 \underline{L}^2$) 3A_2 , 1A_1 , 1E , 3T_1 , and 3T_2 , where the hole-degeneracies are fully taken into account, giving us 376 states. For the case of both the 2+ and 3+ valences, we assume the

truncation of the basis set is justified by the suppression of all other d^n configurations by U_d and all other spin states by the Hund's rule exchange interaction J_d .

The basis sets and the quantum weight distribution for $\text{Co}(\text{NH}_3)_6^{2+}$ and $\text{Co}(\text{NH}_3)_6^{3+}$ are shown in Fig.(6). The next section discusses how parameters were obtained for our model.

C. Determination of model parameters

Most of our model parameters are extracted from single complex calculations with the fully *ab initio* code SIESTA [13] based on density functional theory (DFT). Before discussing the procedure in detail, we briefly want to introduce this code. Nevertheless we want to stress that our way of determining the parameters is quite general and independent of the code one uses as long as it has certain features such as a local atomic basis set and the projected density of states (PDOS).

In running SIESTA we used Troullier-Martins norm-conserving pseudo potentials [31] in the Kleinman-Bylander form [32]. For cobalt, we included spin-polarization and non-linear core corrections [33] to account for a spin-dependent exchange splitting and correlation effects between core and valence electrons, respectively. Relativistic effects are included for the core electrons in the usual scalar-relativistic approximation (mass-velocity and Darwin terms) and by averaging over spin-orbit coupling terms, while no spin-orbit coupling is included for the 4s and 3d valence electrons. Hence spin stays a good quantum number. SIESTA uses a local basis set of pseudo atomic orbitals (PAO) of multiple ζ -type. The first- ζ orbitals are produced by the method by Sankey and Niklewski [34], while the higher- ζ orbitals are obtained from the split valence method well known from quantum chemistry. Polarization orbitals can also be included. We used a double- ζ basis set with polarization orbitals (DZP), as well as the generalized gradient approximation (GGA) in the version by Perdew, Burke and Ernzerhof [35] for the exchange-correlation energy functional. As for the single complex calculations the structures were optimized with the conjugate gradient method until the forces on each atom were below a tolerance of $0.01 \text{ eV}/\text{\AA}$.

We first discuss the estimation of the following parameters, the d-d Coulomb repulsion U_d , Hund's coupling J_d , bare (undressed) d-orbital energy level ϵ_d , the ligand energy level ϵ_L , the ligand-field (purily due to electrostatics) Δ_o , and $10D_q$ which contains contributions from both electrostatics *and* hybridization. In order to get a physical picture of the single complex problem we show the PDOS (DOS projected on atomic 4s, 3 t_{2g} and 3 e_g) of Co(III) in figure 2 as well as Co(II, spin-up) in figure 3 and Co(II, spin-down) in figure 4. All states below the Fermi energy ϵ_F (set to zero) are occupied. One can immediately see the $10D_q$ energy gap between t_{2g} and the anti-bonding \bar{e}_g^* orbitals due to the approximately octra-

hedral symmetry. The π -symmetric t_{2g} orbitals hardly hybridize with the σ -symmetric HOMO of NH_3 while the σ -symmetric e_g orbitals form bonding \tilde{e}_g and anti-bonding \tilde{e}_g^* molecular orbitals (MOs). For further clarification this is schematically illustrated in figure 5. As for Co(II) the non-vanishing total spin ($S=3/2$) introduces spin-dependent MOs due to Hund's coupling, and the partly occupied t_{2g} orbitals split probably due to rhombic distortions. Interestingly, the e_g weights are of similar magnitude in the bonding \tilde{e}_g and the antibonding \tilde{e}_g^* MOs. This indicates the near degeneracy of the e_g and ligand energy level ϵ_d (HOMO of NH_3). In the case of Co(II, spin-up) [see Fig. 3] they are exactly degenerate which provides the ligand energy level $\epsilon_L^{2+} = 0.5(\tilde{e}_g^* + \tilde{e}_g)$ immediately. The t_{2g} and $10D_q$ energies of Co(II/III) can be read off the PDOS, too. In the case of Co(II) we use the weighted average of the t_{2g} peaks. The remaining parameters are estimated as follows.

In order to get the ligand energy level ϵ_L^{3+} of Co(III) we use a simple two-level approximation to describe the mixing of the Co- NH_3 levels. In matrix form this is

$$\begin{pmatrix} e_g & V \\ V & \epsilon_L \end{pmatrix}, \quad (5)$$

where V is the hybridization between the Co e_g levels and the ammine level ϵ_L . Setting the two eigenvalues of Eq. (5) equal to \tilde{e}_g and \tilde{e}_g^* and also constraining the coefficients of the eigenvectors by the weights from the PDOS in figure 2, we obtain ϵ_L^{3+} (as well as V and e_g).

The Coulomb parameters were obtained from a crude mapping assumed between the Kohn-Sham energies obtained from the GGA calculation and a mean-field calculation, where we make use of the single-particle energies of the Co t_{2g} levels

$$\begin{aligned} \tilde{\epsilon}_{t_{2g},\sigma}^{DFT} &\approx \tilde{\epsilon}_{t_{2g},\sigma}^{HF} = \\ \epsilon_d + U_d(N_d - 1) + \frac{J_d}{5}(N_{d\sigma} - N_{d-\sigma}) - \frac{2}{5}\Delta_0 \end{aligned} \quad (6)$$

where ϵ_d is the bare energy (without any electron-electron interaction), $N_{d\sigma}$ are the number of $3d$ electrons with spin σ , N_d is the total number of d -electrons, and Δ_0 is the Madelung (point-charge) contribution to the ligand field. We can write down three equations of this kind, one for Co(III) (spin-independent) and two for Co(II) (one for spin-up and another one for spin-down), and can solve for the three unknowns ϵ_d , U_d , and J_d . The required parameter Δ_0 can be obtained as follows.

Since we know the t_{2g} energies from the PDOS we need to know the e_g energies in order to determine the electrostatic contribution $\Delta_o = e_g - t_{2g}$ for Co(II) and Co(III). These can be extracted in a straightforward way by looking sharply at figure 5 which summarizes all the involved quantities. From the center $\bar{\epsilon} = 0.5(\tilde{e}_g + \tilde{e}_g^*)$ of the bonding \tilde{e}_g and anti-bonding \tilde{e}_g^* MOs and the knowledge of the ligand energy level ϵ_L we obtain $e_g = \bar{\epsilon} + (\bar{\epsilon} - \epsilon_L)$. The resulting point charge contributions to the total ligand-field $10D_q$ are small, $\Delta_o^{2+} = 1.1eV$ and $\Delta_o^{3+} = 0.1eV$.

This is because DFT seems to be biased towards forming rather extended MOs due to an improper treatment of the on-site repulsion among d electrons leading to the well-known deficiency of over-binding [7]. It does not seem to be surprising that $\Delta_o^{2+} > \Delta_o^{3+}$ since due to a 0.2\AA shorter Co-N bond length in the case of Co(III) the hybridization is even larger than for Co(II). Within DFT the $10D_q$ of Co(III) is mainly due to hybridization.

The ability of an electron to transfer from one cobalt ion to the other relies on the hybridization between the HOMO's on the two bridging ligands, which is estimated from the splitting of the HOMO peaks of a two 2 ammine calculation. The amines are in the apex-to-apex orientation. The splitting of the HOMO corresponds to $2t_{inter}$ where we define t_{inter} to be the inter complex NH_3 - NH_3 hopping integral. A similar procedure was applied to obtain the intra complex NH_3 - NH_3 hopping integral t_{intra} between amines of the same complex allowing holes to delocalize among the ligands. The $Co - NH_3$ hybridization V was determined by computing the expectation values $\langle x^2 - y^2 / z^2 | H | HOMO \rangle$ for Co(II) and Co(III) using the HOMO wavefunction from a single ammine and the Hamiltonian matrix of a single complex calculation. Contributions to the hybridization from direct overlap of non-orthogonal d and HOMO wavefunctions were neglected.

Finally, we determine the phonon-coupling constant g and the spring constant K as already outlined in section II. According to Eq. (3) g depends on the Slater-Koster parameter $\eta_{pd\sigma}$. It is determined by setting $V_{pd\sigma} = V$ from the DFT method. As for K we use the experimental Co-ligand stretching frequencies, $357cm^{-1}$ for Co(II) and $494cm^{-1}$ for Co(III) [36].

The parameters are summarized in Table I. Therefore we can write down an effective Hamiltonian that includes only these frontier orbitals: the set of Co $3d$ orbitals and the NH_3 HOMO states. We use the Hamiltonian of Eq.(1) as the effective Hamiltonian for each of the single cobalt hexaammine complexes, the 2+ and 3+ nominal valences. The d -electron parameters ϵ_d , U_d , J_d , the ligand-field splitting $10D_q$, etc. all refer to the cobalt $3d$ electrons, while the ligand label L refers to the ammine HOMO. We would like to solve for the groundstates of $Co(NH_3)_6^{2+/3+}$ within this model.

IV. RESULTS AND DISCUSSION

A. Quantum weights of single complexes

The model Hamiltonian we constructed is diagonalized on the many-electron basis we have described using the set of parameters presented in Table I. We show the results in Fig.(6).

For $Co(NH_3)_6^{2+}$, there is 71.5% in the $hs-3d^7$ (4T_1) state and 28.1% in the corresponding $3d^8\bar{L}^2$ where an electron has transferred from the NH_3 HOMO to the e_g shell of the Co atom. This weight is actually distributed

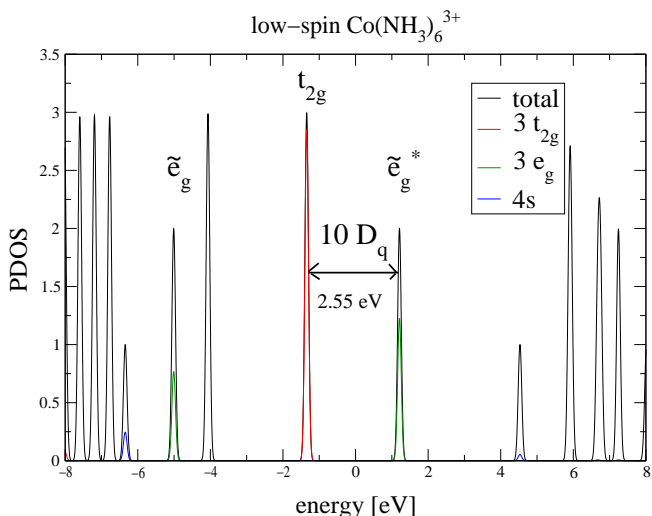


FIG. 2: Projected density-of-states (PDOS) of low-spin Co(III) ($d^6, S = 0$) for spin-up and spin-down. The Fermi energy $\epsilon_F = -11.82\text{eV}$ is set to zero.

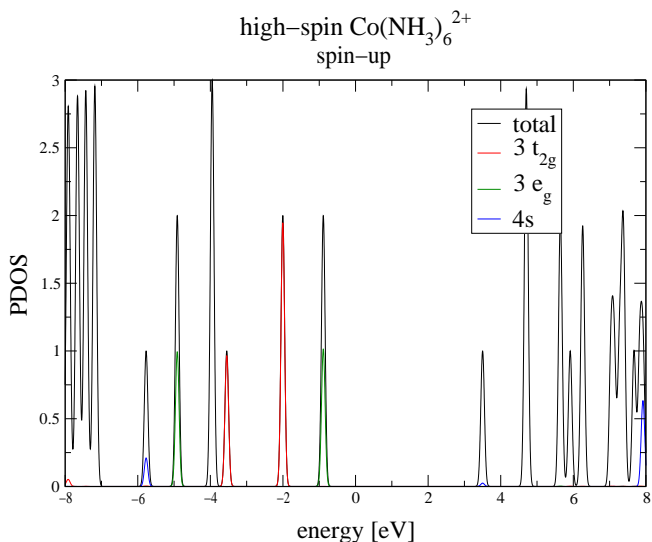


FIG. 3: PDOS of high-spin Co(II) ($d^7, S = 3/2$). The spin-up part is shown. The Fermi energy $\epsilon_F = -5.77\text{eV}$ is set to zero.

with $\sim 5\%$ on each of the six coordinated ammine ligands. This distribution of quantum weight is due to the $\text{NH}_3\text{-NH}_3$ hybridization we included on our model. One may picture the hole as delocalized or *smear*ed over the first solvation shell. The fact that only a small fraction of the hole resides on any one ligand has important implications for the charge-transfer process and we will discuss this later. The remainder of the quantum weight resides in the $1s\text{-}3d^7$ (2E), which is small since it mixes into the groundstate by the weak spin-orbit coupling. The vertical energy separation $E({}^2E - {}^4T_1)$ is 1.18 eV (9513 cm^{-1}), which is in good agreement with *ab initio* calculations.

For $\text{Co}(\text{NH}_3)_6^{3+}$, the vertical energy separation $E({}^3T_1 - {}^1A_1)$ is too small ($\sim 0.5\text{ eV}$) when compared with

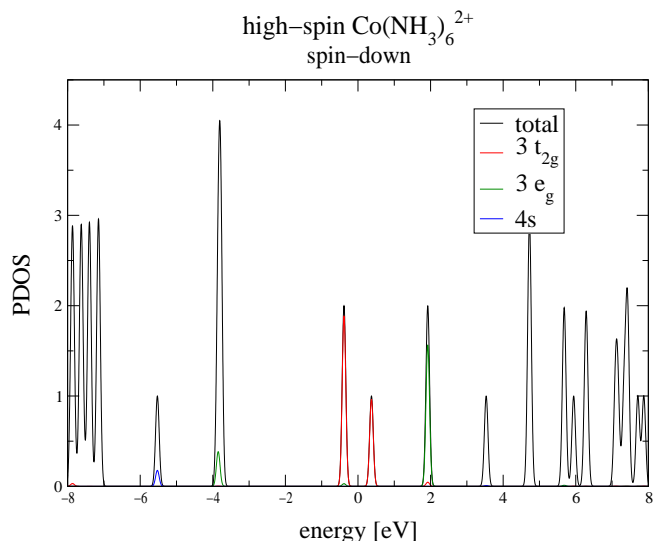


FIG. 4: PDOS of high-spin Co(II) ($d^7, S = 3/2$). The spin-down part is shown. The Fermi energy $\epsilon_F = -8.17\text{eV}$ is set to zero.

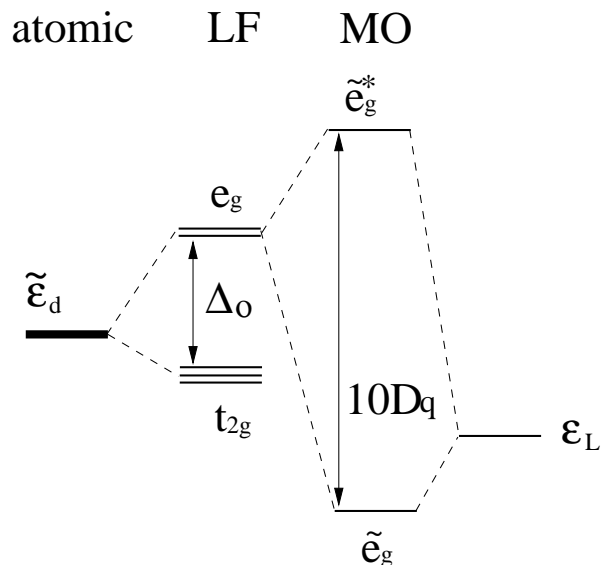


FIG. 5: Ligand-field (LF) and molecular orbital (MO) pictures.

experiment ($\sim 1.7\text{ eV}$) for the set of parameters. A parameter that we have some freedom with is the ligand-field splitting $10Dq$. The lack of constraint on $10Dq$ emerges from the model not taking proper account of all of the contributions to the ligand-field energy splitting. $10Dq$ is composed of the point-charge ligand-field Δ_0 and a contribution due to the hybridization of the cobalt and ligand orbitals. While the model does take into account the most important hybridization between the e_g and ammine HOMO, it *does not* actually form bonding/anti-bonding pairs since the $3d$ electron sector

TABLE I: Parameters determined for hexaammine cobalt complexes from SIESTA calculations. (1) and (2) refer to in-plane and axial ligands, respectively. All parameters except g_γ (eV/Å) and K (eV/Å²) are in units of eV.)

Parameters	Co(II)	Co(III)
ϵ_d	-33.9	-33.9
U_d	4.1	4.1
J_d	-2.0	-2.0
g_γ	-3.8	-5.2
K	48.0	92.0
ξ	0.09	0.09
$10Dq$	1.6	2.6
ϵ_H	-11.1	-14.4
$V(x^2 - y^2 - L)$	1.9	2.8
$V(z^2 - L)$ (1)	-1.1	-1.6
$V(z^2 - L)$ (2)	-2.1	-3.2

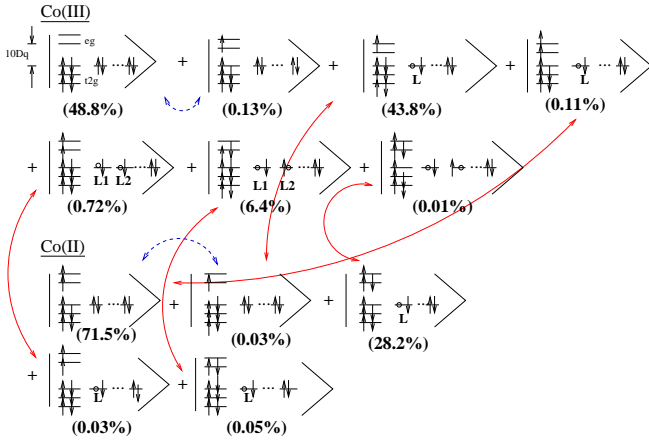


FIG. 6: Many-body groundstates of $\text{Co}(\text{NH}_3)_6^{3+}$ and $\text{Co}(\text{NH}_3)_6^{2+}$. The quantum weights are the squared expansion coefficients of the groundstate eigenvector $|\alpha_i\rangle^2$ on the restricted Hilbert space. The red arrows indicate states that would couple through the bridge Hamiltonian. The blue arrows show coupling through the spin-orbit term. There are 65 basis states for $\text{Co}(\text{NH}_3)_6^{2+}$ and 376 for $\text{Co}(\text{NH}_3)_6^{3+}$.

of our basis set is represented in the atomic orbital basis, i.e. the e_g levels are just the atomic orbitals, so in the current treatment we cannot accurately predict the hybridization contribution. Therefore, we treat the ligand-field splitting as a free-parameter in our model. While the $10Dq$ value seems to work well for $\text{Co}(\text{NH}_3)_6^{2+}$ it does not reproduce the correct vertical energy separation between low-spin and $S = 1$ $3d^6$, so by increasing it by 1 eV to 3.55 eV, we recover the vertical energy from experiment. The effect on the weights is to shift $\sim 5\%$ from $ls-3d^7$ to $ls-3d^6$, as would be expected.

We now need to determine if and how the effects of correlation between the d electrons manifest in this system. For $\text{Co}(\text{NH}_3)_6^{3+}$, the hole seems nearly fully delocalized between the first coordination sphere of amines and the cobalt $3d$ shell with 51% in the $ls-3d^6$ (1A_1) configuration

and 42% in the $ls-3d^7\bar{L}$ states. This weight is divided up with $\sim 7\%$ per state with a hole localized in one of the six NH_3 HOMO's. At first glance, the physical picture appears to be very much like the screening cloud associated with the Kondo effect. In the case of cerium materials, the hole left behind from an electron hopping from the conduction band to the $4f$ impurity delocalizes over the entire continuum of conduction states, dynamically screening the local moment and leading to the formation of the singlet bound state.

We cannot say if the appreciable hole-weight delocalized over the ligands is due to mixed valence state or not. Both the $ls-3d^6$ (1A_1) and $ls-3d^7$ (2E) states possess filled diamagnetic t_{2g} shells, so the Hund's rule exchange contribution to the $d-d$ Coulomb interaction is equal in each case. Since we only have two configurations, we may shift the Fermi level to correspond with the $ls-3d^7$, therefore we do not have to refer to U_d . From this perspective, the delocalization of the hole between metal $3d$ and the ammine orbital looks simply like the consequence of single-particle covalency. This interpretation is also consistent with the composition of molecular orbitals from our *ab initio* calculations which show nearly equal contributions from metal and ligand orbitals in the (e_g - σ) bonding/anti-bonding pair.

However, there does seem to be an analogy between the d^6 , $d^7\bar{L}$, and $d^8\bar{L}^2$ configurations of $\text{Co}(\text{NH}_3)_6^{3+}$ and the configurations f^0 , $f^1\bar{L}$, and $f^2\bar{L}^2$ of the mixed valence rare-earth compounds such as CeO_2 and metallic α -Ce, where mixed valence has been established. In both the transition metal and lanthanide cases these multiple configurations mix into the groundstate because of their near-degeneracy. In both cases there is also large suppression of the two ligand-hole states due to the Hubbard- U Coulomb repulsion of electrons on the localized impurity levels. In the cerium materials the f^1 electron and the ligand hole \bar{L} can form an exciton-like bound-state that preserves the symmetry of the diamagnetic f^0 state, i.e. a spin-singlet state with no orbital moment. In $\text{Co}(\text{NH}_3)_6^{3+}$, we would have a similar energy lowering associated with freezing out the 2-fold orbital degeneracy of the e_g shell and the spin-degree of freedom, antiferromagnetically coupled to the hole delocalized over the six NH_3 HOMO levels.

Such a state usually forms if the singly-occupied configuration is slightly lower in energy than the empty level. This requirement is not satisfied in $\text{Co}(\text{NH}_3)_6^{3+}$ since the diamagnetic $3d^6$ state is stabilized by 1.6 eV with respect to the $ls-3d^7$ configuration. However, the hybridization between the e_g and ammine HOMO's are large enough (~ 2 -3 eV) to mitigate this energy gap. In CeO_2 the partial occupancy of the $4f$ -level is observed to be ~ 0.6 , consistent with the lattice volumes that are somewhat shorter than expected for Ce^{3+} compounds. In $\text{Co}(\text{NH}_3)_6^{3+}$, if this type of partial occupancy exists (~ 0.5 from our model calculation), experimentalists should observe bond lengths that are somewhere intermediate between those expected for $\text{Co}(\text{NH}_3)_6^{2+}$ and $\text{Co}(\text{NH}_3)_6^{3+}$.

For $\text{Co}(\text{NH}_3)_6^{2+}$, as stated above, the values for the single-particle Co $3d$ and ammine HOMO energies are such that there is almost complete resonance, and molecular orbitals are constructed with $\sim 50\%$ of each type of orbital. We observe in our calculated result the effect of the large U_d in suppressing the $3d^8$ weight so the admixture is now on the order of $\sim 70\%$ of the hole is localized in the d shell, while $\sim 30\%$ is delocalized over the ammine ligands. This suppression of $3d^8$ configurations is expected. The question is what consequence do these effects have on the electron transfer matrix element H_{DA} .

B. Construction of Born-Oppenheimer Potential Energy Surfaces and Estimate for H_{DA}

We performed calculations of the groundstates for the single $\text{Co}(\text{NH}_3)_6^{2+}$ and $\text{Co}(\text{NH}_3)_6^{3+}$ complexes. We would now like to use the basis sets of both of these complexes to form an encounter complex that represents the reactants in the electron-transfer process.

We connect the single $2+/3+$ complexes in the apex-to-apex orientation through a bridge composed of amines from each molecule, which gives us the Hamiltonian

$$H = h_1 + h_2 - t \sum_{\sigma} (c_{LA\sigma}^{\dagger} c_{RA\sigma} + h.c.) \quad (7)$$

Both h_1 and h_2 refer to the identical model Hamiltonian for each single complex given by Eqn.(1). The third term describes hole tunneling through the ligand bridge composed of the two amines in close contact. The creation operator $c_{LA\sigma}^{\dagger}$ refers to the creation of a σ -spin hole on the left NH_3 ligand (belonging to $\text{Co}(\text{NH}_3)_6^{2+}$) and $c_{RA\sigma}^{\dagger}$ is the corresponding operator for the right ammine (belonging to $\text{Co}(\text{NH}_3)_6^{3+}$). The hopping integral t can be estimated by noting that $2t$ is approximately the energy splitting between the bonding/anti-bonding orbitals formed from the HOMO of each of the two bridging NH_3 , oriented by close contact of the hydrogen atoms of each ammine. We must now solve for the groundstate using the appropriate basis set. We construct this by taking a tensor product of our basis sets for $\text{Co}(\text{NH}_3)_6^{2+}$ and $\text{Co}(\text{NH}_3)_6^{3+}$. The basis set is doubled to account for exchanging $\text{Co}(\text{NH}_3)_6^{2+}$ and $\text{Co}(\text{NH}_3)_6^{3+}$ in space. There is then another multiplication by two in order to treat the Hermitian matrix in order to use diagonalization routines suited for real, symmetric matrices [37]. So the basis set is then of rank

$$N = 376 \times 65 \times 2 \times 2 = 97760. \quad (8)$$

Given that most routines scale as $\sim N^3$, where N is the dimensionality of the Hilbert space, conventional routines, even on very fast machines (~ 4 GHz microprocessor) would make single-point calculations very time-consuming. Given that we would like to sample the $2D$ groundstate energy surface as a function of the breathing

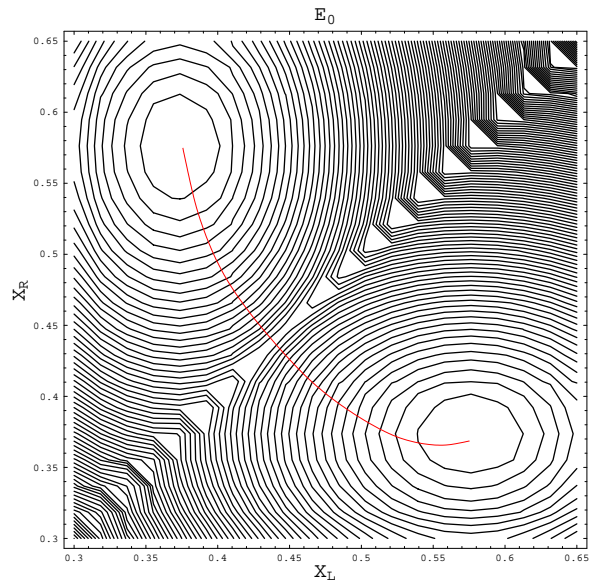


FIG. 7: The Born-Oppenheimer potential energy surface for the $\text{Co}(\text{NH}_3)_6^{2+/3+}$ self-exchange electron transfer reaction. Only the inner-sphere contribution is shown. The groundstate energy was plotted on a 40×40 grid using a Lánczos diagonalization routine to diagonalize the 97760^2 eigenvalue problem. The contour level spacing is chosen to be 0.03 eV/level. x_L and x_R are the reaction coordinates corresponding to the totally symmetric metal-ligand stretching mode. The transition state, defined as the saddle point along $x = x_L = x_R$ is at $x = 0.44 \text{ \AA}$. The difference in the Co-N bond length between $\text{Co}(\text{II})$ and $\text{Co}(\text{III})$ is 0.2 \AA .

coordinates for each complex, x_L and x_R at the resolution needed to accurately determine the transition state, we need very efficient matrix diagonalizer. Plotting this potential energy surface is a computationally intensive problem.

The solution was to implement a Lánczos matrix-diagonalization routine, which scales as order N [38] since it involves only matrix-vector multiplication for sparse matrices. The Lánczos algorithm converts a large $N \times N$ matrix into a tridiagonal $m \times m$ matrix ($m \leq N$). It uses a three-term recurrence relationship which requires one trial groundstate vector to start the sequence. The eigenvectors tend to become parallel during iteration of the procedure. Since we are not interested in them for this application, a costly ($\sim N^3$) reorthogonalization step does not have to be implemented.

The plot in Fig.(9) is a two-dimensional contour plot representing the Born-Oppenheimer potential energy surface we have plotted solving the 97760^2 eigenvalue problem 1600 times.

The oval shape of the minima are consistent with a larger force constant (narrower potential) for $\text{Co}(\text{NH}_3)_6^{3+}$. The horizontal and vertical distances between the minima correspond to $\sim 0.2 \text{ \AA}$ which agrees well with the experimentally measured difference in the

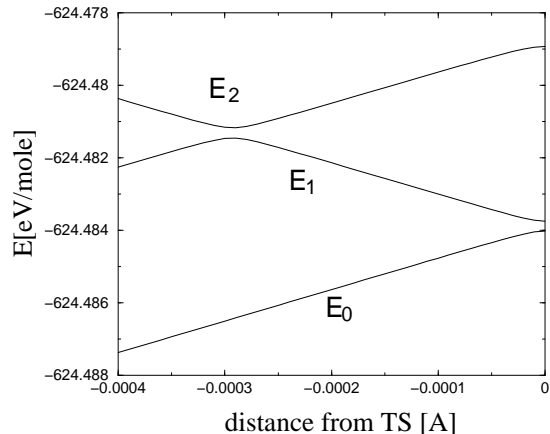


FIG. 8: Cross-section of PES from Fig.(7) along the reaction coordinate $d=x_L-x_R$ close to the TS. The energy splittings ($2|H_{DA}|$) between the groundstate E_0 and first excited state E_1 at the TS (0\AA) is about 2 cm^{-1} . The splitting between E_1 and E_2 at $d=-2.8\times 10^{-4}\text{\AA}$ has a similar value.

metal-ligand distance between the 2+ and 3+ forms of the hexaammine cobalt complex. The donor surface **D** for the ET corresponds to the encounter complex $\text{Co}(\text{NH}_3)_5^{3+}(\text{NH}_3)-(\text{H}_3\text{N})\text{Co}(\text{NH}_3)_5^{2+}$, which is given by the parabola in the upper left corner. The acceptor surface **A** is that of $\text{Co}(\text{NH}_3)_5^{2+}(\text{NH}_3)-(\text{H}_3\text{N})\text{Co}(\text{NH}_3)_5^{3+}$ and is the lower right parabola in Fig.(7). The transition state is the cusp feature at $x=0.44\text{\AA}$ and corresponds to a narrowly-avoided crossing between the **D** and **A** diabatic surfaces. The electronic coupling opens a gap equal to $2|H_{DA}|$ between **D** and **A** at the crossing point, where H_{DA} is the electronic coupling factor.

The general method of extracting H_{DA} is as follows: We find the TS by plotting the energy along the diagonal x in Fig.(7) with high resolution. The TS is the saddlepoint at $x=0.44\text{\AA}$. We then read off the difference between the first excited and ground states. H_{DA} is half of this difference.

On the other hand, one can exploit that H_{DA} is also a groundstate property. Instead of calculating the excited state, one can obtain it from calculating the energy difference between the groundstate adiabatic surface evaluated at the TS and the avoided crossing between the diabatic **D** and **A** surfaces that results when the bridge hopping integral t is turned off.

In Fig.(10) we plot a cross-section of PES from Fig.(9) along the reaction coordinate $d = x_L-x_R$ in the region of the TS. The energy splittings ($2|H_{DA}|$) between the groundstate E_0 and first excited state E_1 at the TS (0\AA) is $\simeq 2\text{ cm}^{-1}$. The splitting between E_1 and E_2 at $d=-2.8\times 10^{-4}\text{\AA}$ has a similar value. The splittings between E_0 and E_1 and also E_1 and E_2 originate from lifting of the degeneracy of the components of the 4T_1 irreducible representation of Co(II) by the spin-orbit coupling.

Our result ($\sim 2\text{ cm}^{-1}$) is smaller than Newton's calculation of H_{DA} , which gave 9.5 cm^{-1} from *ab initio* calcu-

lations. We have essentially reproduced this calculation from our simpler model. What the reduction of $|H_{DA}|$ implies is that the correlation effects we have observed in the single complexes of cobalt hexaammine do not seem to enhance the ET rate. The reason is that we still rely on states that couple through the spin-orbit coupling, most noticeably $ls-3d^7({}^2E)$ for the $\text{Co}(\text{NH}_3)_6^{2+}$ complex. The quantum weight of this state in the groundstate is not increased by the correlation-induced suppression of $3d^8$ occupancy. In fact, this suppression tends to reduce the magnitude of H_{DA} . The arrows in Fig.(2) indicate that the $3d^8$ states of both $\text{Co}(\text{NH}_3)_6^{2+}$ and $\text{Co}(\text{NH}_3)_6^{3+}$ couple through the bridge term of H . The weight on these states is small because of the large U_d value.

V. CONCLUSIONS

We have introduced a variant of the Anderson Impurity Model that is appropriate for describing the valence electronic structure of TM molecules. We have coupled this model to a metal-ligand stretching mode. We have applied this model to investigate the effect of strong correlations among the cobalt $3d$ electrons on the self-exchange electron transfer rate in the cobalt hexamines $\text{Co}(\text{NH}_3)_6^{2+/3+}$.

We have constrained the model parameters by using the results of *ab initio* density functional theory calculations and experimental stretching frequencies. The single-particle hybridizations V_{dL} were extracted directly and the Coulomb parameters (ϵ_d, U_d, J_d) were obtained from mapping to a mean-field solution of our model. Using these parameters, we found the groundstates of both 2+ and 3+ nominal valences. For the $\text{Co}(\text{NH}_3)_6^{3+}$ state we find strong configurational admixture between the $3d^6$ and $3d^7\bar{L}$ states. The hole \bar{L} is fully delocalized between the cobalt atom and the first coordination sphere of amines. While this resembles the screening cloud and partial occupancy of the impurity level seen in mixed valent compounds like CeO_2 , the large $3d^7\bar{L}$ weight could simply be a purely single-particle effect since the delocalization is consistent with the equal metal and ligand orbital composition of molecular orbitals near the Fermi level from the DFT calculation. For $\text{Co}(\text{NH}_3)_6^{2+}$ there is an obvious signature of the effect of large U_d , with a suppression of $\sim 20\%$ of the quantum weight on $3d^8\bar{L}^2$ states.

We couple the complexes together by a bridging Hamiltonian to form the encounter complex and generate a basis set by using the tensor product of the single hexaammine basis states. This gives a very large eigenvalue problem ($N \simeq 10^5$) that is solved using Lanczos methods. The groundstate energy surface is plotted, resolving the two minima of the electron transfer process. We are able to extract the electronic coupling H_{DA} as the energy lowering at the transition state, relative to the diabatic surfaces. What we found is that configurational admixture does not enhance H_{DA} and we get a result $\sim 4\text{ cm}^{-1}$, that is within a factor of 5 of Newton's original calcula-

tion.

It appears that the disparity of two orders of magnitude in the self-exchange electron transfer rate of $\text{Co}(\text{NH}_3)_6^{2+/3+}$ cannot be explained on the basis of the electronic structure of a single complex. One aspect that has been completely ignored in this calculation are solvation effects beyond the first coordination shell. While one would expect, in the gas phase, that the single, symmetric breathing coordinate would be an excellent approximation to the breathing coordinate, solvent effects could significantly change the height of the barrier by adding anharmonicity to the potential wells. This could contribute to the adiabatic nature of the reaction.

Another possible source of enhancement for the ET rate could be through *dynamical* effects. The dynamical prefactor depends on the details of how the system crosses and recrosses the thermal barrier. The presence of the low-lying spin-orbit states that are separated from the groundstate by very small ($\sim 1 \text{ cm}^{-1}$) energies could give the vibronic wavepacket multiple channels for reaching the other minimum. This is a possibility that can be explored with our model, which provides fast "on-the-fly" sampling of the correct electronic structure. Excited state calculations of the bimetallic TM active site involving open-shell states, coupled by the TM atom spin-orbit interaction, would be very difficult to do with state-of-the-art quantum chemistry codes.

Finally, it is possible that the relevant Born-

Oppenheimer surfaces at the transition state are different from those at equilibrium, which we have explored elsewhere within DFT theory[16]. In particular, an intermediate spin surface appears to be thermally accessible and favorable at the transition state. In that paper we actually found a rate two orders of magnitude *faster* than experiment. It is interesting to note that within our calculation and Newton's UMP2 calculation[18] the electron correlation effects actually *reduce* the transition rate. Within our variational state treatment the reason is clear: Coulombic blocking effects eliminate a class of determinants which can facilitate charge transfer. It will be interesting to explore the effects of correlations upon the intermediate spin manifold of states.

The method proposed in this paper could be applied to other TM systems such as the active sites in metalloproteins. More elaborate ways of coupling the electronic sector to the protein structure will have to be devised but the efficiency and simplicity of our method might be very useful in identifying transition state configurations.

Acknowledgements We have benefitted from useful discussions with M. Newton. This work was supported by the United States Department of Energy, Office of Basic Energy Sciences, Division of Materials Research. M.X.L. has been supported by a UC Davis NSF NEAT-IGERT graduate fellowship and the Laboratory Directed Research and Development program at Los Alamos National Laboratory.

-
- [1] D.T. Richens, *The Chemistry of Aqua Ions* (John Wiley and Sons, 1997).
- [2] L.J. Kagen, *Myoglobin: Biochemical, Physiological, and Clinical Aspects* (Columbia University Press, 1973).
- [3] *Proceedings of the International Conference on Valence Fluctuations*, edited by E. Muller-Hartmann, B. Roden, and D. Wohlleben (North-Holland, Amsterdam, 1985).
- [4] Y. Guo, J.-M. Langlois, and W.A. Goddard III, *Science* **239**, 896 (1988).
- [5] For a recent overview, see K. Hirao, K., Ed. *Recent Advances in Multireference Methods; Recent Advances in Computational Chemistry, Vol. 4* (World Scientific: Singapore, 1999).
- [6] I.N. Levine, *Quantum Chemistry*, 3rd Edition, (Allyn and Bacon, 1983).
- [7] Ibério de P.R. Moereira, F. Illas, R.L. Martin, *Phys. Rev. B* **65**, 155102 (2002).
- [8] K.M. Rosso and J.R. Rustad, *J. Phys. Chem. A*, **104**, 6718 (2000).
- [9] L. Rulišek and Z. Havlas, *J. Chem. Phys.* **112**, 149 (2000).
- [10] G.A. Sawatzky, J.W. Allen, *Phys. Rev. Lett.* **53** 24 2339 (1984).
- [11] O. Gunnarsson, K. Schönhammer, *Phys. Rev. B* **28** 4315 (1983).
- [12] C.M. Varma and Y. Yafet, *Phys. Rev. B* **13** 2950 (1976).
- [13] D. Sánchez-Portal, P. Ordejón, E. Artacho, and J. M. Soler, *Int. J. Quantum Chem.* **65**, 453 (1997); E. Artacho, D. Sánchez-Portal, P. Ordejón, A. Garcia, and J. M. Soler, *Phys. Status Solidi (b)* **215**, 809 (1999); P. Ordejón, E. Artacho, and J. M. Soler, *Phys. Rev. B* **53**, R10441 (1996).
- [14] M. Gerloch, *Magnetism and Ligand-Field Analysis*, (Cambridge University Press, 1983).
- [15] C.J. Margulis, V. Guallar, E. Sim, R.A. Friesner, and B.J. Berne, *J. Phys. Chem. B*, **106**, 8038 (2002).
- [16] R.G. Endres, M.X. LaBute, D.L. Cox, *J. Chem. Phys.* **118**, 8706 (2003).
- [17] S. Larsson and K. Stahl, *Inorg. Chem.* **25** 3033 (1986).
- [18] M.D. Newton, *J. Phys. Chem.* **95** 95 (1991).
- [19] M.X. LaBute, R.V. Kulkarni, R.G. Endres, and D.L. Cox, *J. Chem. Phys.* **116**, 3681 (2002).
- [20] R.H. Austin, K. Beeson, L. Eisenstein, H. Frauenfelder, I.C. Gunsalus, V.P. Marshall, *Phys. Rev. Lett.* **32**, 403 (1974).
- [21] W. P. Su, J. R. Schrieffer, and A. J. Heeger, *Phys. Rev. B* **22**, 2099 (1980).
- [22] J.C. Slater and G.F. Koster, *Phys. Rev.* **94**, 1498 (1954).
- [23] W.A. Harrison, *Electronic Structure and the Properties of Solids* (W.H. Freeman, New York, 1980), pp. 450-451 and Table A-1.
- [24] D.E. Richardson and P. Sharpe, *Inorg. Chem.*, **30**, 1412 (1991).
- [25] H. Taube, *Electron Transfer Reactions of Complex Ions in Solution*, Academic Press, New York (1970), R.G. Linck, *MTP Int. Rev. Sci.: Inorg. Chem., Ser. One*, **9** (1971), N. Sutin, in *Inorganic Biochemistry*, Vol. **2** Chapter 19, G.L. Eichhorn, Ed., Elsevier, New York (1973),

- D. Geselowitz and H. Taube, *Adv. Bioinorg. Mech.* **1** 391 (1982), B.S. Brunschwig, C. Creutz, *et. al.*, *Faraday Discuss. Chem. Soc.* **74**, 113 (1982).
- [26] E. Buhks, *et. al.*, *Inorg. Chem.* **18** 7 (1979).
- [27] L.E. Orgel, *10th Conf. Inst. Int. de Chimie, Rapports et Disc.*, Inst. Solvay, Brussels, 289 (1956).
- [28] M.D. Newton, *J. Phys. Chem.* **90**, 3734 (1986).
- [29] M.D. Newton, *Coordination Chemistry Reviews* **238**, 167 (2003).
- [30] N. Sutin, *Prog. Inorg. Chem.* **30** 441 (1983).
- [31] N. Troullier and J. L. Martins, *Phys. Rev. B* **43**, 1993 (1991).
- [32] L. Kleinman and D. M. Bylander, *Phys. Rev. Lett.* **48**, 1425 (1982).
- [33] S. G. Louie, S. Froyen, and M. L. Cohen, *Phys. Rev. B* **26**, 1738 (1982).
- [34] O. F. Sankey and D. J. Niklewski, *Phys. Rev. B* **40**, 3979 (1989).
- [35] J. P. Perdew, K. Burke, and M. Ernzerhof, *Phys. Rev. Lett.* **77**, 3865 (1996).
- [36] J. F. Endicott, B. Durham, and K. Kumar, *Inorg. Chem.* **21**, 2437 (1982); and references therein.
- [37] <http://www.ulib.org/webRoot/Books/NumericalRecipes/bookc.html>
- [38] J.K. Cullum and R.A. Willoughby, *Lanczos algorithms for large symmetric eigenvalue computations*, eds. S. Abarbanel et al (Birkhäuser, Boston, Basel, Stuttgart, 1985); N.S. Sehmi, *Large order structural eigenanalysis techniques*, (Ellis Horwood Limited, Chichester, 1989).